

B. STRUCTURE OF NUCLEI NEAR, AT AND BEYOND THE PROTON DRIPLINE

The program to explore the structure and stability of nuclei along the proton dripline continues to be a forefront theme in our nuclear structure research. It has many interesting facets, both for astrophysical processes and for extending our understanding of the structure and stability of nuclei. It provides a natural bridge that connects contemporary research with future projects which exploit radioactive beams. The unique combination of Gammasphere, arguably the world's premier gamma-ray detector, with the Argonne Fragment Mass Analyzer, arguably one of the world's most productive spectrometers for far-from-stability channel selection, has opened up a new domain for research. In addition, the superb qualities of the ATLAS accelerator in beam selection, timing and emittance, has enhanced the performance of other channel selection devices like microball and neutron detectors giving them greater sensitivity for low cross-section physics. Prompt spectroscopy of gamma-rays emitted from fission fragments still provides unique data on very neutron rich nuclei, and using the combination of Gammasphere and our "in-house" radiochemistry resources, this program was pursued vigorously. In the future, Coulomb excitation of beams of exotic nuclei will be an important tool. In preparation, we are developing techniques for high-efficiency measurements of beam excitation.

b.1. Alignment Delays in Even-Even $N = Z$ Nuclei (C. J. Lister, M. P. Carpenter, A. M. Heinz, D. J. Henderson, R. V. F. Janssens, J. Schwartz, D. Seweryniak, I. Wiedenhöver, J. Cizewski,* N. Fotiadis,* A. Bernstein,† J. A. Becker,† R. Bauer,† P. E. Garrett,† S. Vincent,‡ A. Aprahamian,‡ P. Hausladen,§ D. Balamuth,§ and S. M. Fischer¶)

We have investigated $N = Z$ ^{72}Kr , ^{76}Sr and ^{80}Zr , which all have well-deformed rotational sequences, to investigate backbending, or alignment effects which normally occur shortly above $J = 8$ (or a rotational frequency near $\hbar\omega = 0.5$ MeV). Using Gammasphere, Microball, and the FMA we considerably extended the decay schemes of these nuclei into the region of interest. All show evidence that the alignments of $g_{9/2}$ particles are different from their $N = Z + 2$ and $N = Z + 4$ neighbors. ^{72}Kr is particularly striking. It has an alignment which is very delayed when compared to its neighbors. ^{76}Sr shows a much more modest delay, and we can only place a limit that ^{80}Zr has a delay, as the

yrast sequence seems smooth to the highest observed spin. Thus, an experimental verification that a delay occurs was made. Figure I-12 shows the kinematic and dynamic moments of inertia for $N = Z$ and $N = Z + 2$, $N = Z + 4$ isotopes of Kr, Sr and Zr. A letter presenting these measurements is accepted for publication¹. While the experimental facts now seem clear, the meaning of these observations is still open to interpretation. It is certainly true that the alignment mechanism is very sensitive to shape and to normal $T = 1$ pairing, so extraction of unambiguous information on np-pairs and their coupling schemes seems difficult.

*Rutgers University, †Lawrence Livermore National Laboratory, ‡University of Notre Dame, §University of Pennsylvania, ¶DePaul University

¹S. M. Fischer et al., Phys. Rev. Lett. (2001).

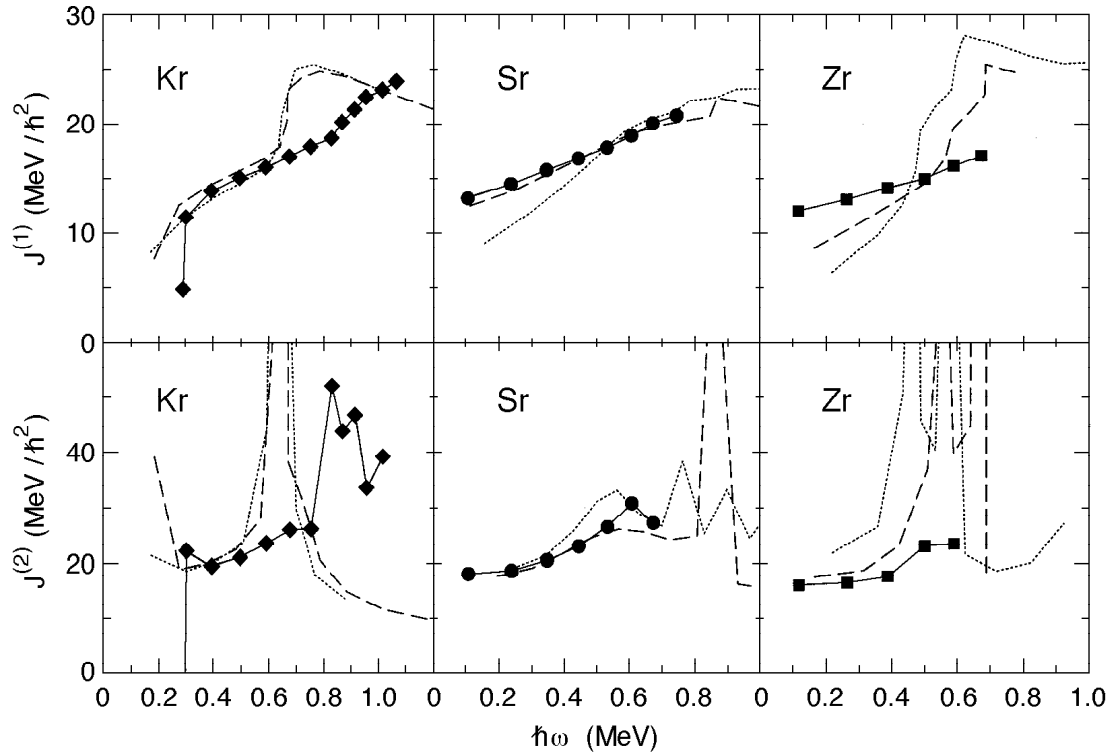


Fig. I-12. The kinematic and dynamic moments of inertia for $N = Z$ and $N = Z + 2$, $N = Z + 4$ isotopes of Kr, Sr and Zr.

b.2. Structure of $N = Z$ Odd-Odd Nuclei, Including ($N = Z = 35$ ^{70}Br) (C. J. Lister, D. G. Jenkins, T. A. Sienko,* D. Balamuth,† S. M. Fischer,‡ P. Fallon,§ A. O. Macchiavelli,§ D. G. Sarantites,¶ and W. Reviol¶)

It was observed that most heavy odd-odd $N = Z$ nuclei have a ground-state spin of $J = 0$, arising from coupling of the last pair of nucleons to an anti-symmetric $T = 1$ wavefunction. This state may just be a coupling of the last pair of particles, or may reflect a more collective ground state of a $T = 1$ pair field with contributions from many configurations. If the latter is true a “pair-gap” should exist, just as in even-even nuclei, pulling this state down and leaving few, or no nearby low-lying levels. The location of the $T = 1$ states, relative to other configurations with $T = 0$ and coupled to $J = 1 \dots 2j$ are sensitive to both long and short range np-interactions. Thus, studying $N = Z$ odd-odd nuclei is pertinent to the question of np-pairing in general. ^{70}Br is an interesting case, as it lies in the middle of the fp-g-shell and has $N = Z$ neighbors which are quite well understood as having substantial oblate groundstate deformation.

In practice, the experimental identification of levels in the odd-odd $N = Z$ nuclei proved quite difficult, and several unsuccessful attempts were made to identify

them. Traditionally, to investigate low excitation, low spin states, a light ion reaction would be optimal. However, the nuclei of interest lie far from stability, so heavy-ion reactions must be used. To constrain heavy ion reactions to populate low-spin states is not easy, and very careful selection of the reaction and beam energy is essential. Even in the best conditions, the population cross-sections are small, about 150 μbarns for ^{70}Br , so all the latest techniques are needed, including the use of Gammasphere. ^{70}Br was recently found to have a low-lying $J = 9$ β -decaying isomer which further hampers the population of low-lying states. We used the $^{40}\text{Ca}(^{32}\text{S},\text{pn})^{70}\text{Br}$ reaction at 80,85,90 and 100 MeV to investigate this nucleus at low spin. An array of neutron detectors was used to select the reaction channel. The experiment was optimized for identification of low energy gamma-rays; many odd-odd nuclei in the region have many transitions < 100 keV. An array of LEPS detectors was used, which was sensitive to photons as low as 20 keV, and Gammasphere operated in its “low-threshold mode” to

increase sensitivity for gamma rays below 200 keV. The more strongly produced ^{70}Se was used as a template to measure the entry spin distribution and verify the correct beam energy was used. Online analysis indicated that 85 MeV beam energy led to maximum production of the two-nucleon evaporation channels, and the mean entry spin was below $J = 8$. Considerable progress in developing the decay scheme was made. A set of $T = 1$ analogs to ^{70}Se states were identified, together with several low energy transitions which are candidates for the expected magnetic dipole decays between $T = 0$ and $T = 1$ states. Although lifetimes were not measured, the E2 vs M1 branching ratios of states which are analog to ^{70}Se levels were determined, and establish that the M1 decays are strong, with matrix elements much larger than expected for isoscalar decays between $T = 0$ states. These M1 decays clearly allow the relative isospin of states to be measured. High spin cascades of states built on the $J =$

9 isomer are also undergoing analysis: they were populated in the $^{40}\text{Ca}(^{36}\text{Ar},\alpha\text{pn})^{70}\text{Br}$ reaction. At present two new sequences have been found.

In the theoretical domain three avenues are being explored. For low spin configurations, we are working in collaboration with J. Stone (Oxford) on a two-quasiparticle-deformed core coupling calculation. Further, the IBM-4 model of van Isacker (GANIL) which includes np-bosons, is being tested. Fig. I-13 shows a comparison of low spin states with the IBM-4 predictions which were performed prior to the experiment. This should help interpretation of the paired regime, and the strength of np-correlations. At the highest spin, A. Afanasejv (Notre Dame) is working on an unpaired rotating-mean-field calculation, which should help identify the highest spin configurations, through their changes of moment of inertia near termination.

*Purdue University Calumet, †University of Pennsylvania, ‡DePaul University, §Lawrence Berkeley National Laboratory, ¶Washington University

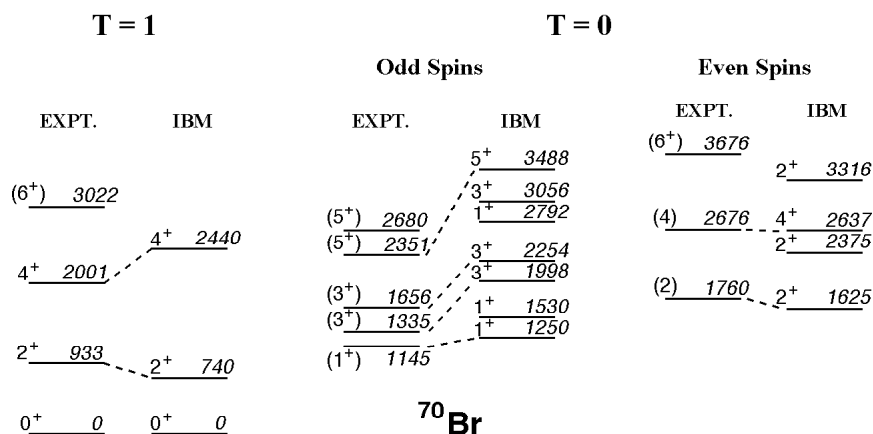


Fig. I-13. The low-lying levels of ^{70}Br determined from this work compared to the np-interacting boson model, IBM-4.

b.3. New Results in Proton Radioactivity (C. N. Davids, A. Heinz, G. L. Poli, D. Seweryniak, † T. Davinson, * H. Mahmud, * J. J. Ressler, ‡ K. Schmidt, * J. Shergur, ‡ A. A. Sonzogni, § W. B. Walters, ‡ and P. J. Woods*)

Proton and alpha emission from ^{185}Bi were confirmed and measured with improved statistics. The ^{185}Bi nuclei were produced via the $^{95}\text{Mo}(^{92}\text{Mo},\text{pn})$ reaction at a bombarding energy of 420 MeV. The proton decay energy from the $1/2^+$ intruder state in ^{185}Bi to the ^{184}Pb ground state was measured to be 1.598(16) MeV with a proton branching ratio $b_p = 0.85(6)$. An alpha decay branch from the same state was measured, $b_\alpha = 0.15(6)$, with an energy of 8.08(3) MeV. The state

has a half-life of 50(8) μs . In addition, the alpha branching ratio of the ground state of ^{184}Pb was determined for the first time to be $b_\alpha = 0.23(14)$.

The deformed proton emitter ^{117}La was observed, confirming its previous discovery by the Legnaro group¹. It was produced via the $^{64}\text{Zn}(^{58}\text{Ni},\text{p}4\text{n})$ reaction. We observe a single proton peak at 806(5)

keV, with a half-life of 24(3) ms. Data analysis is continuing.

Several new odd-odd proton emitters were observed, increasing the data base on these relatively rare species. One case is deformed and two are in the spherical region. The deformed emitter is ^{130}Eu , made via the

$^{58}\text{Ni}(^{78}\text{Kr}, p5n)$ reaction. It has a proton energy of 1027(14) keV, and a half-life of 0.90(+61-16) ms. The spherical emitters are ^{164}Ir [$E_p = 1778(13)$ keV, $t_{1/2} = 58(+46-18)\mu\text{s}$] and ^{170}Au [$E_p = 1712(8)$ keV, $t_{1/2} = 0.48(+47-16)\text{ms}$]. In the case of ^{164}Ir , this brings to 4 the number of Ir isotopes that are proton emitters. Data analysis on these emitters is continuing.

*University of Edinburgh, United Kingdom, †Argonne National Laboratory and University of Maryland,

‡University of Maryland, §Brookhaven National Laboratory

¶F. Soramel *et al.*, Phys. Rev. C **63**, 031304(R) (2001).

**b.4. Identification of Excited Structures in Proton Unbound Nuclei $^{173,175,177}\text{Au}$:
Shape Co-Existence and Intruder Bands** (F. G. Kondev, K. Abu Saleem,* I. Ahmad, H. Amro,† M. P. Carpenter, C. N. Davids, A. Heinz, R. V. F. Janssens, T. L. Khoo, T. Lauritsen, C. J. Lister, G. L. Poli, J. Ressler,|| D. Seweryniak,|| I. Wiedenhöver, J. A. Cizewski,‡ M. Danchev,§ D. J. Hartley,§ W. C. Ma,¶ W. Reviol,** L. L. Riedinger,§ and M. B. Smith‡)

Beyond the proton-drip line, nuclei are energetically unbound to proton emission ($Q_p > 0$), a decay mode that often occurs in competition with α decay. The decay rates, which depend on the tunneling probability through the Coulomb barrier, are sensitive to the energy and the angular momentum of the emitted particle as well as to the quantum numbers and intrinsic configurations of the states involved in the parent and daughter nuclei. Consequently, proton decay has become an important spectroscopic tool to study nuclear structure at the very limit of nuclear existence. In many instances, the experimental half-lives can be understood in terms of predictions based on the WKB approximation. Such calculations were shown to be inadequate in describing proton decay in nuclei such as ^{131}Eu and ^{141}Ho and the discrepancies are attributed to the presence of sizable prolate deformation¹. In the region near the intersection of the $Z = 82$ shell closure and the proton dripline, the effects of deformation on the properties of proton emitters may also be expected: the phenomenon of shape coexistence at low spin and excitation energy was observed in many nuclei and the interaction between configurations associated with different shapes should influence the decay rates. However, the experimental situation is unclear because the degree in which this coexistence persists in drip line nuclei is poorly known.

We observed, for the first time, excited structures in the ^{173}Au ($N = 94$), ^{175}Au ($N = 96$) and ^{177}Au ($N = 98$) isotopes. These nuclei provide the opportunity to elucidate the shape driving properties of proton excitations based on the important $h_{9/2}$, $f_{7/2}$ and $i_{13/2}$ proton orbitals in a region where they were not investigated extensively, e.g. below mid-shell ($N \sim 104$). In addition, the role of the low- Ω $i_{13/2}$ neutrons can also be examined. The impact of the latter

configuration on the formation of different minima has been largely neglected in this mass region. All three Au isotopes are energetically unbound to the emission of protons.

Excited states in ^{173}Au , ^{175}Au and ^{177}Au were populated via the $p2n$ channels in fusion reactions of ^{84}Sr ions with ^{92}Mo (at 390 and 395 MeV beam energy), ^{94}Mo (380 and 385 MeV) and ^{96}Mo (380 MeV) targets. Prompt γ rays were detected with the Gammasphere array in conjunction with the recoil-decay tagging technique. Partial level schemes showing the yrast structures of ^{173}Au , ^{175}Au and ^{177}Au are presented in Fig. I-14. A common feature in all three cases is the presence of an α -decaying, high-spin isomer. The measured α -decay energies and half-lives were found to be in agreement with the most recently published values, but in general the present results are of greater accuracy. The isomers are assigned $\pi = 11/2^-$ and the $11/2^- [505] (h_{11/2})$ Nilsson configuration. A low spin isomer was also observed in ^{173}Au and ^{177}Au , but not in ^{175}Au .

Sample γ -ray spectra showing transitions depopulating states in ^{173}Au , ^{175}Au and ^{177}Au are given in Fig. I-15. At high spin, the yrast line of ^{177}Au comprises of a well-deformed prolate band. While intensity considerations established an E2 multipolarity for the 160.1 keV transition ($\alpha_T(\text{exp}) = 0.70(7)$; $\alpha_T(\text{E1}) = 0.13$, $\alpha_T(\text{E2}) = 0.84$, $\alpha_T(\text{M1}) = 1.97$), other in-band transitions are assumed to be of E2 character. Below the $(13/2^+)$ level, the intensity flux splits into two branches, one proceeding via the 319.4, 289.9 and 240.8 keV transitions through the $(9/2^-)$ member

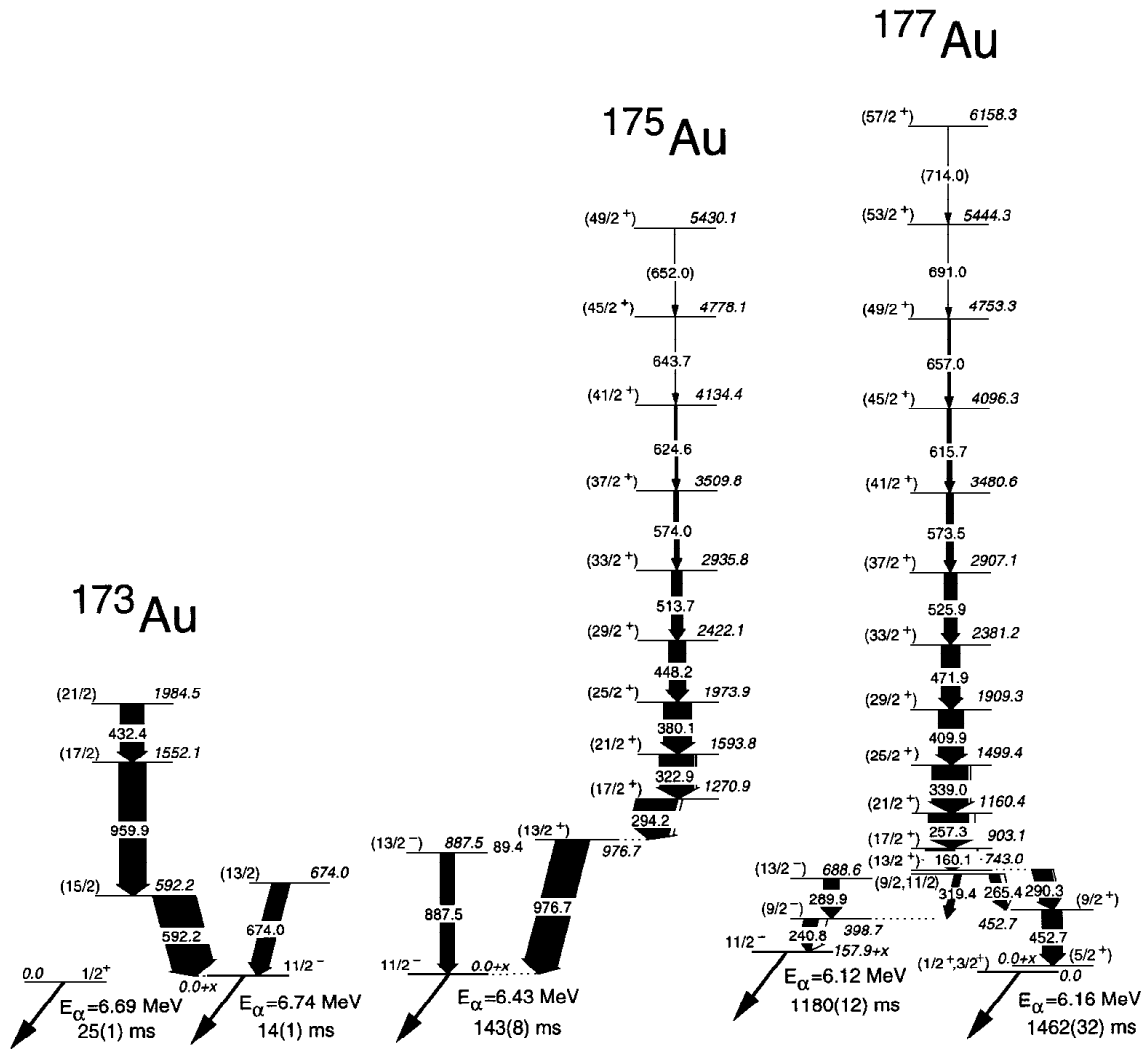


Fig. I-14. Partial level scheme for the yrast cascades in ^{173}Au , ^{175}Au and ^{177}Au . The width of the arrows is proportional to the intensity of the transitions. The α -decaying states are indicated with the corresponding energies and half-lives.

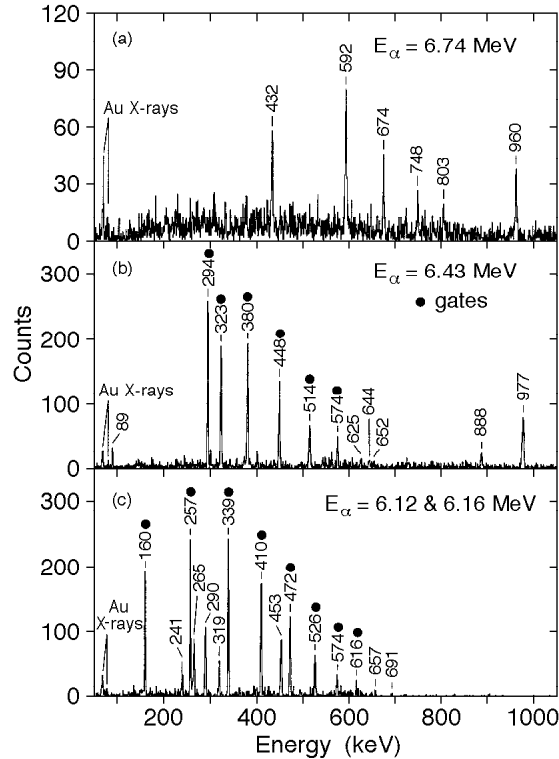


Fig. I-15. (a) Spectrum of γ rays correlated with the ^{173}Au α -decay line of $E_{\alpha} = 6.74$ MeV. Summed, background-subtracted γ -ray coincidence spectra from the α - γ - γ matrix produced by gating on the $E_{\alpha} = 6.43$ MeV (^{175}Au) line (b) and on the $E_{\alpha} = 6.12$ and 6.16 MeV (^{177}Au) lines (c). The transitions used as gates are indicated with filled circles.

of the $\pi h_{9/2}$ band and the $11/2^-$ isomer, while the other reaches the $(1/2^+, 3/2^+)$ isomer via the 265.4, 290.3, and 452.7 keV γ rays. The yrast line of ^{175}Au is also formed by a collective band, similar to that seen in ^{177}Au , but its decay proceeds entirely through the $11/2^-$ isomer. The E1 character of the 89.4 keV transition follows from intensity balance considerations, and other in-band transitions are assumed to be stretched quadrupoles. In contrast to ^{175}Au and ^{177}Au , no sign of collectivity is observed in ^{173}Au .

Positive parity yrast bands are known in the heavier odd-mass Au and Tl nuclei. They were associated with a prolate shape and assigned the intruder $1/2^+[660]$ ($i_{13/2}$) proton configuration. A characteristic feature of these structures is strong Coriolis mixing which leads to large alignments and sizable signature splitting, with only the favored signature being observed. The newly established bands in ^{175}Au and ^{177}Au are consistent with such an interpretation.

Experimental alignments for the positive parity sequences in ^{175}Au and ^{177}Au are compared with those of their even-even platinum cores in Fig. I-16. The observed values of alignment for the bands in

$^{175,177}\text{Au}$ are consistent with expectations for a rotationally-aligned $i_{13/2}$ proton, and support the $1/2^+[660]$ configuration assignment. At the lowest frequencies, the Pt nuclei show an increase in alignment caused by a change from an oblate to a more deformed prolate shape. The yrast sequence in ^{175}Au exhibits a related behavior, thus suggesting that a similar shape change may have occurred. This is also evident from the spectrum shown in Fig. I-15b, where the 294.2 keV transition does not follow the regular collective pattern established by the higher-energy transitions and, therefore, cannot be interpreted as a member of the rotational cascade. In addition, a variable moment of inertia (VMI) fit applied to the levels between $(17/2^+)$ and $(49/2^+)$, predicts an energy of about 199 keV for the $17/2^+ \rightarrow 13/2^+$ in-band transition. In this mass region an oblate to prolate shape change is a well-established phenomenon. It occurs along the positive-parity yrast structures in the heavier odd-Z $^{185,187,189}\text{Tl}$ isotopes. In fact, while the $1/2^+[660]$ ($i_{13/2}$) prolate band was observed to be yrast at high spin in these nuclei, the lowest $13/2^+$ state was assigned to the $13/2^+[606]$ ($i_{13/2}$) oblate configuration. Taking into account the striking similarities between the present observations for ^{175}Au and these

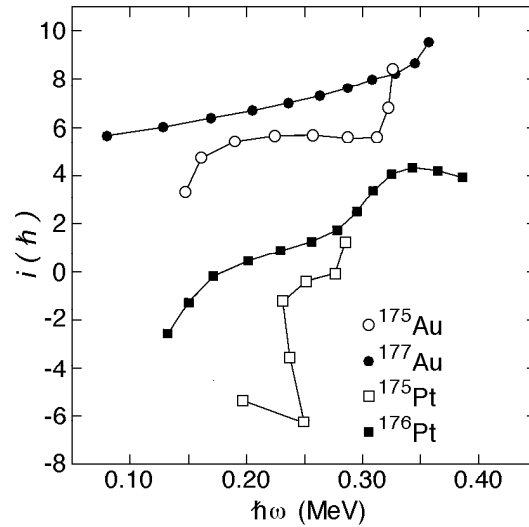


Fig. I-16. Aligned angular momenta for the yrast bands in ^{175}Au and ^{177}Au , and their even-even Pt core nuclei. The same reference parameters, $\mathfrak{S}_0 = 27.5 \text{ MeV}^{-1} h^2$ and $\mathfrak{S}_1 = 190.0 \text{ MeV}^{-3} h^4$, have been used for all bands.

positive-parity T1 sequences, the same $13/2+[606]$ oblate configuration is proposed for the $(13/2+)$ state at 976.7 keV. In terms of shape co-existence, it is worth noting that structures associated with three different shapes compete for yrast status in ^{175}Au . A near-spherical ground state ($1\pi = 11/2^-$) is followed by the $(13/2+)$ oblate level while the prolate band dominates at higher spins. The energy separation between the observed states can be associated with the energy difference between these minima, albeit the excitation energy of the prolate well is more subtle since the $i_{13/2}$ prolate band is not observed down to its bandhead (presumably due to effects associated with deformation and Coriolis mixing).

The so-called VMI fit was carried out for the $i_{13/2}$ bands in $^{175,177}\text{Au}$, as well as for those of the heavier odd-mass gold isotopes. Empirical values of the deformation were subsequently deduced using $\beta_2 \approx 91.7 Q_0/(ZA^{2/3})$, with a quadrupole moment estimated as $Q_0 \approx 39.4(\mathfrak{S}_0)^{1/2}$, where \mathfrak{S}_0 is the moment of inertia. The results are presented in the upper part of Fig. I-17, together with predictions given by total Routhian surface (TRS) calculations based on a Woods-Saxon potential. It is apparent that the deformation of the $i_{13/2}$ band in ^{177}Au is larger than that in ^{175}Au : such a difference would account for the larger alignment observed for the former band (see Fig. I-16). By extrapolating the trend seen in Fig. I-17a towards lower neutron number, one would expect an even smaller deformation for the $i_{13/2}$ band in ^{173}Au , a

structure which was not observed in the current work. It is also interesting to note that while the TRS predictions placed the maximum in deformation near mid-shell, the extracted empirical values maximize at lower neutron number ($N \sim 98-100$). The reason for such a difference is at present not fully understood. It is interesting to speculate that this may be due in part to changes in the shell structure associated with weak binding. On the other hand, it is worth pointing out that, at $N = 98$, the neutron Fermi level resides at the boundary of a deformed ($\beta_2 \sim 0.25$) sub-shell gap and that this results in an increased shell-stability for specific prolate configurations.

In order to gain further insight into the differences in deformation noted above, calculations of the single-particle quadrupole moments and of the occupation probabilities of various orbitals were carried out using a Woods-Saxon potential with the Lipkin-Nogami treatment of pairing. Figure I-18 shows the contribution of specific orbitals to the deformation of the $i_{13/2}$ bands in $^{173,175,177}\text{Au}$. The importance of the $1/2-[541] (h_9/2)$ orbital in the formation of the prolate minimum was noted before and is also evident in Fig. I-18a. The correlation between the change in deformation with neutron number and the occupation of the low- Ω $i_{13/2}$ neutrons is also apparent. Hence, one may conclude that the decrease in deformation of the $i_{13/2}$ bands in the odd-mass Au nuclei with neutron number is at least partially due to the step-wise decrease in the occupations of the low- Ω $i_{13/2}$ neutron orbitals, as well as to the $h_9/2$ proton orbital.

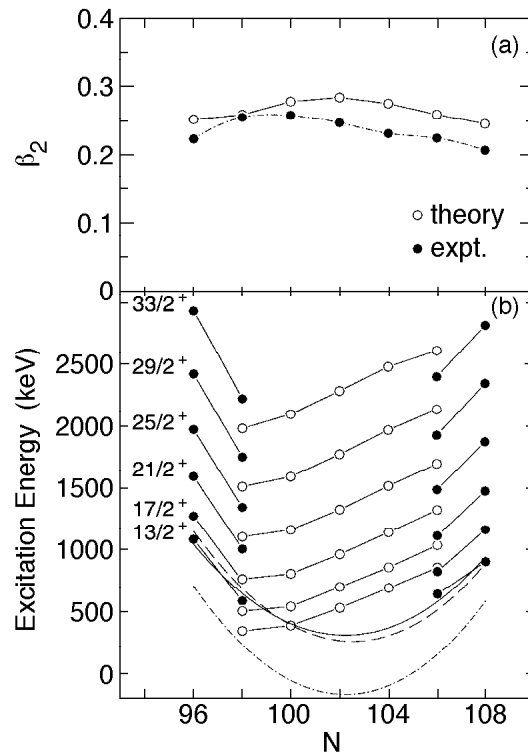


Fig. I-17. (a) Equilibrium deformations for the $1/2+[660] (i_{13/2})$ configuration over a range of gold isotopes. The filled symbols correspond to the values deduced from the VMI fit, while the open symbols are predictions from TRS calculations (see text for details). (b) Energy systematics for the prolate $1/2+[660] (i_{13/2})$ band in the odd-mass Au isotopes relative to the $11/2^- (h_{11/2})$ intrinsic state (filled symbols) and the $9/2^-$ member of the $h_{9/2}$ band (open symbols). The position of the $13/2^+$ level in ^{175}Au has been deduced from the VMI fit, as discussed in the text. The parabolic fit for the $\pi i_{13/2} - \pi h_{11/2}$ energy differences in the Au isotopes are shown by the solid line. The dashed and the dot-dashed lines represent fits to the prolate-oblate energy differences in the neighboring even-even Hg and Pt isotopes, respectively.

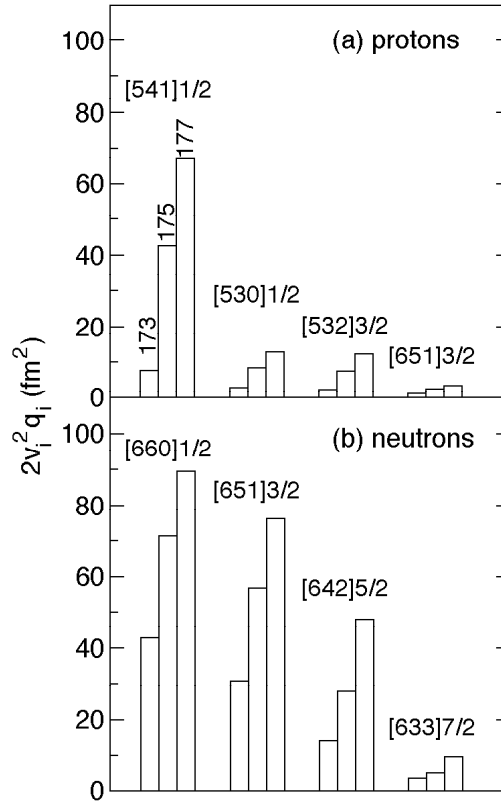


Fig. I-18. Predicted contributions of the main intruder proton (a) and neutron (b) orbitals to the quadrupole deformation of ^{173}Au (left bin), ^{175}Au (middle) and ^{177}Au (right) nuclei. The single-particle quadrupole moments (q_i) and energies were calculated using the Woods-Saxon potential with "universal" parameterization and deformations $\beta_2 = 0.170$ (^{173}Au), $\beta_2 = 0.223$ (^{175}Au) and $\beta_2 = 0.255$ (^{177}Au) ($\beta_4 = -0.005$ in all cases). The occupation probabilities, v_i , were calculated using the Lipkin-Nogami treatment of pairing with $G_\nu = 18.0/A$ (MeV) and $G_\pi = 20.8/A$ (MeV). In the calculation procedure the proton $1/2^+[660]$ ($i_{13/2}$) orbital was occupied (blocked), thus having an occupational probability of unity.

Figure I-17b compares the excitation energies of the $1/2^+[660]$ ($i_{13/2}$) band members relative to the $11/2^-(h_{11/2})$ and the $9/2^-(h_{9/2})$ states in several odd-mass gold isotopes. The parabolic fit to the $\pi i_{13/2}$ (prolate)- $\pi h_{11/2}$ (near-spherical/weakly-deformed) energy differences shows a minimum near mid-shell and resembles closely the prolate-oblate energy differences observed in neighboring even-even Pt and Hg isotopes. Another feature shown in Fig. I-17b is that the $\pi i_{13/2}$

(prolate)- $\pi h_{9/2}$ (prolate) energy difference continues to decrease below mid-shell. Such a behavior should not be a surprise, given the deformation differences between these two orbitals. It should also be noted that the effects of Coriolis coupling and triaxiality were not taken explicitly into account in the systematics shown in Fig. 4b, although their role may be significant as the deformation reaches smaller values.

*Argonne National Laboratory and Illinois Institute of Technology, †Argonne National Laboratory and Mississippi State University, ‡Rutgers University, §University of Tennessee-Knoxville, ¶Mississippi State University, ||Argonne National Laboratory and University of Maryland, **University of Tennessee-Knoxville and Washington University-St. Louis

IC. N. Davids *et al.*, Phys. Rev. Lett. **80**, 1849 (1998).

b.5. Measurements of g-Factors of Excited States in Zr and Mo Nuclei Using γ Rays from Secondary Fission Fragments (I. Ahmad, M. P. Carpenter, J. P. Greene, R. V. F. Janssens, F. G. Kondev, T. Lauritsen, C. J. Lister, D. Seweryniak, D. Patel,* A. G. Smith,* R. M. Wall,* J. F. Smith,* G. S. Simpson,* O. J. Onakan,* B. J. P. Gall,† and O. Dorveaux†)

An experiment was performed to measure the g-factors of excited states in neutron-rich fission fragments through the time-integral perturbed angular correlation functions between pairs of secondary-fragment γ rays. The experiment involved the use of a ^{252}Cf source of total activity 100 μCi sandwiched between two layers of iron foil. Prior to the deposition of the californium, the iron metal foils (each 15 mgcm^{-2} thick) were annealed in an oven at 650° C for ten minutes. The magnetization of these foils as a function of applied field was measured using a magnetometer. The results of this measurement showed that the magnetic moment of the iron reached saturation of its calculated maximum value at 0.1 T. The californium was then electroplated onto the surface of one of the iron foils and a layer of indium metal (200 μgcm^{-2} thick) evaporated over a second iron foil. The layer of indium acted as an aid to adhesion¹ between the active foil and the second foil, which was rolled on top to produce a closed source in which the fission fragments stop in iron. The source was placed within a vacuum chamber at the center of the Gammasphere array. A pair of small, permanent magnets applying a field of 0.2 T were placed either side of the source in the direction normally reserved for the beam to Gammasphere. The direction of the applied field could be reversed by rotating the magnet assembly through 180°. This field change was performed every few hours over the course of a two week run. Approximately 10^{10} events comprising three or more γ rays were collected.

Determinations of g-factors have been made using measurements of time-integral, perturbed angular correlation functions. Unlike the data obtained in a previous Euroball experiment with a gadolinium foil², in which the analysis method depended on a small

precession-angle approximation, these data show large precessions in the light fission fragments. The analysis technique has had to be modified to fit double ratios corresponding to the full perturbed angular correlation function over the whole Gammasphere array. The application of this new method has worked well. Preliminary results for the lowest 2+ states in several Zr and Mo fragments are presented in Table 1.

Where there are existing g-factor measurements in the literature, notably in the strongly populated ^{100}Zr and ^{104}Mo , our measurements show consistency with the established values. Due to an ambiguity in the double ratios, the 2+ state in ^{102}Zr has two possible solutions with almost identical χ^2 values. At present it is difficult to decide between the two solutions to the fit. One gives a higher than expected g-factor, the other much lower than expected. In addition, the error on the lifetime of this state is large, contributing to uncertainty in the g-factor. Estimating the lifetime of this state with a recently measured quadrupole moment at spin ~ 10 suggests that it could be much greater than the estimate quoted below - possibly as high as 4 ns. This would imply that the -1896 mRad precession is the most likely solution as the g-factor would then be +0.36 - close to the Z/A value of +0.39 for this nucleus. A measurement of the g-factor for the 4+ state in the same rotational band is in progress and should resolve the ambiguity. In the Mo isotopes, there appears to be a trend towards decreasing g-factors, suggested by previous measurements and supported by this work.

In addition to the results presented here, measurable precessions were observed from this data set for 2+ states in Pd, Ru, Ba, Ce and Nd even-even isotopes.

*University of Manchester, United Kingdom, †IREs Strasbourg, France

1C. Teich, A. Jungclaus, and K. P. Lieb, Nucl. Instrum. Methods **A418**, 365 (1998).

2A. G. Smith *et al.*, Phys. Lett. **B453**, 206 (1999).

3G. Rao, Hyperfine Interactions **24**, 1119 (1985).

TABLE 1. Preliminary results of the g-factor measurements. The impurity hyperfine field strengths are taken from the compilation³.

	$I\pi$	Energy (KeV)	τ (ns)	B (Tesla)	Experimental ϕ_p (mRad)	Experimental g	g (other)
98Zr	2+	1223	<0.289	-27.4(4)	-72(31)	>+0.190(86)	
100Zr	2+	213	0.779(28)		-217(12)	+0.213(14)	+0.22(5)
102Zr	2+	152	2.76(36)		-1896(177)	+0.525(85)	
	2+	152			-250(23)	+0.069(11)	
102Mo	2+	296	0.180(6)	-25.6(1)	-59(18)	+0.268(82)	+0.42(7)
104Mo	2+	192	1.04(6)		-283(14)	+0.222(17)	+0.19(11)
106Mo	2+	172	1.803(43)		-289(19)	+0.131(9)	
108Mo	2+	193	0.72(43)		-205(46)	+0.232(149)	

b.6. Few Particle Excitations of the N = 83 Isotones ^{134}Sb and ^{135}Te (I. Ahmad, M. P. Carpenter, R. V. F. Janssens, T. L. Khoo, T. Lauritsen, C. J. Lister, P. Reiter, D. Seweryniak, I. Wiedenhöver, P. J. Daly,* P. Bhattacharyya,* C. T. Zhang,* Z. W. Grabowski,* B. Fornal,† R. Broda,‡ and J. Blomqvist‡)

The spectroscopic studies of ^{134}Sb and ^{135}Te , which have two and three valence nucleons, respectively, outside the doubly magic ^{132}Sn , are the prime source of information about empirical neutron-proton interactions in an important region of neutron-rich nuclei. We have made measurements to study the structure of neutron-rich nuclei using the Gammasphere array and a ^{248}Cm fission source. A pellet made of ^{248}Cm and KCl, with an activity of $\sim 6 \times 10^4$ fissions/sec, was placed in the center of the Gammasphere at Argonne, which consisted of 99 Compton-suppressed germanium detectors. The event trigger required detection of at least four gamma rays within an 800-ns time interval, with the storage of time and energy information for every gamma ray registered. The data were collected over a period of 10 days and were subsequently analyzed off-line by using the technique of gamma matrices and gamma cubes.

New transitions in ^{134}Sb were identified by double gating on one line in the complementary partners, ^{112}Rh , ^{111}Rh and ^{110}Rh and the other the 2124 keV

gamma ray in ^{134}Sb . These and other double gates allowed us to construct the level scheme shown in Fig. I-19. Most of the levels above 4 MeV in ^{134}Sb identified in the present work appear to be members of a multiplet connected by low energy transitions. An exception is the level at 4570 keV, which decays by high energy gamma rays only. We make an assignment of $(\pi h_{11/2} \nu i_{13/2})_{12^-}$ configuration. The relative energies of the $(\pi g_{7/2} \nu i_{13/2})_{10^+}$ and $(\pi h_{11/2} \nu i_{13/2})_{12^-}$ two-particle states in ^{134}Sb were estimated using empirical proton-neutron interactions extracted from the counterpart $(\pi h_{9/2} \nu j_{15/2})_{12^+}$ and $(\pi i_{13/2} \nu j_{15/2})_{14^-}$ configurations in ^{209}Bi , with mass scaling as $A^{-1/3}$. The calculated level energy separation of 2393 keV is in fairly good agreement with the experimental value of 2136 keV. The level energies in ^{134}Sb calculated by the above prescription are included in Fig. I-19. The level schemes of ^{135}Te were also calculated in the same way and were found to agree with the experimental data. The results of this investigation were published.¹

*Purdue University, †IFJ Cracow, Poland, ‡Royal Institute of Technology, Stockholm, Sweden
1B. Fornal and R. Broda, Phys. Rev. C **63**, 024322 (2001).

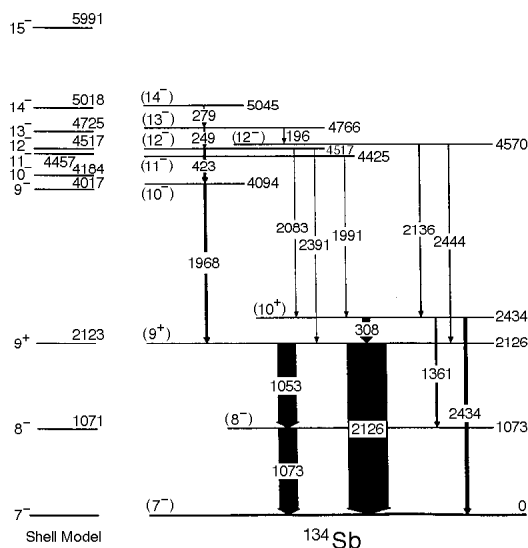


Fig. I-19. The level scheme of ^{134}Sb deduced in the present study. Arrow widths are proportional to the relative transition intensities. Level energies calculated by the shell model described in the text are shown on the left side.

b.7. Coulomb Excitation of $^{124,126}\text{Xe}$ Studied with Segmented Germanium Detectors

(M. P. Carpenter, C. J. Lister, D. Henderson, R. V. F. Janssens, D. G. Jenkins, F. Kondev, T. Pennington, W. F. Mueller,* I. Wiedenhöver,* J. C. Church,* D. C. Dinca,* J. Enders,* T. Glasmacher,* P. A. Lofy,* H. Olliver,* B. C. Perry,* B. T. Roeder,* and A. Gade†)

Six 32-fold segmented germanium detectors of the Michigan State University germanium array were used in an experiment at ATLAS for the first time. The elements were placed around the target to form an array of ~6% photopeak efficiency at 1.3 MeV and with a segment opening angle of $\sim 10^\circ$. Figure I-20 shows a photograph of the experimental arrangement. Beams of both ^{124}Xe and ^{126}Xe were scattered off a Ni target and detected in the ANL large-area four-Quadrant PPAC. Due to the granularity of the germanium array, it is possible to study γ -ray emission from the Coulomb excited recoiling nuclei with high resolution and efficiency. The Xe isotopes have been of interest for many years because their level structure approach the O6-symmetry of the Interacting Boson Model. However, there are crucial observable quantities which are missing in many of these studies that include $B(E2)$ values for transitions decaying from yrast and non-yrast low spin states. These measurements would provide a

stringent test of models. In the present measurement, the ground bands were observed up to 8^+ , and the gamma band up to the 6^+ level. Mixed symmetry states involving both neutron and proton excitations are also interesting. With regard to the isovector 2^+ state, preliminary analysis indicates that it is collective, however, the analysis is proceeding in order to quantify this result. Although this was a “shakedown” test of the equipment, publishable results are expected.

Early in 2001, it is planned to place the experimental setup behind the FMA focal plane. The goal of the upcoming experiment will be to Coulomb excite radioactive ^{176}Os ions produced at the FMA target position, mass selected by the FMA, and scattered off a Ni-foil positioned ~ 1 meter behind the focal plane. If this experiment proves successful, there are plans to utilize the MSU array in this same configuration near the end of 2001.

*Michigan State University, †University of Cologne, Germany

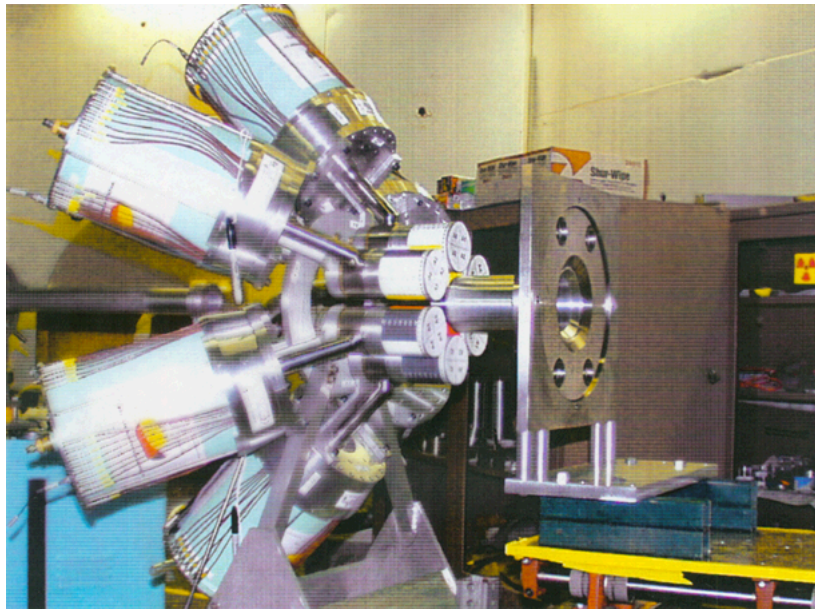


Fig. I-20. MSU segmented germanium array in "close packed" geometry for Coulomb excitation of Xe beams.

